I&EC research
Industrial & Engineering Chemistry Research

Article

pubs.acs.org/IECR

Simultaneous Optimization of Working Fluid and Process for Organic Rankine Cycles Using PC-SAFT

M. Lampe,[†] M. Stavrou,[‡] H. M. Bücker,[§] J. Gross,[‡] and A. Bardow*[,†]

[†]Institute of Technical Thermodynamics, RWTH Aachen University, 52062 Aachen, Germany

[‡]Institute of Thermodynamics and Thermal Process Engineering, Universität Stuttgart, 70569 Stuttgart, Germany

[§]Institute for Computer Science, Friedrich Schiller University, 07737 Jena, Germany

ABSTRACT: Organic Rankine Cycles (ORCs) generate power from low temperature heat. To make the best use of the diverse low temperature heat sources, the cycle is tailored to each application. The objective is to maximize process performance by optimizing both process parameters and the working fluid. Today, process optimization and working fluid selection are typically addressed separately in a two-step approach: working fluids are selected using heuristic knowledge; subsequently, the process is optimized. Such an approach can lead to suboptimal solutions, since the optimal fluid might be excluded by the heuristics. We therefore present a framework for the holistic design of ORCs enabling the simultaneous optimization of the process and the working fluid based on process performance. The simultaneous optimization is achieved by exploiting the rich molecular picture underlying the PC-SAFT equation of state in a continuous-molecular targeting approach (CoMT-CAMD). To allow for the prediction of caloric properties, a quantitative structure−property relationship (QSPR) for the ideal gas heat capacity is proposed that relies on pure component parameters of PC-SAFT. The framework is used for the optimization of a geothermal ORC in a case study. A sound holistic design of process and working fluid is achieved.

1. INTRODUCTION

The Organic Rankine Cycle (ORC) enables the valorization of low temperature heat by converting it into power. Low temperature heat is available from various sources, such as waste heat,[1] solar,[2] and geothermal[3] applications. Each application has its unique specifications regarding temperature and mass flow rate of the heat carrier, and for cooling of the ORC.

To enable optimal process performance, the ORC process has to be tailored to the specific application. Tailoring involves process optimization and selection of a working fluid. Depending on the application and the decision maker, the objective of the optimization can be based on criteria from thermodynamics (e.g., first or second law efficiency,[3,4] net power output[3,5]) or economics (e.g., cost of energy[6,7]).

Working fluid selection is generally recognized as a crucial decision in the design of an ORC, since the performance of the cycle directly depends on the thermophysical properties of the working fluid.[2,8−10] However, as the thermophysical properties of the working fluid influence the optimal process parameters in a complex way, working fluid selection today still depends on experience and heuristic knowledge. Thus, systematic methods for working fluid selection are desired. Quoilin et al.[11] recently showed in their review that different studies recommend different working fluids for the same temperature levels. The selection of different working fluids can be due to either different objective functions or different sets of preselected working fluids. Quoilin et al.[11] therefore conclude that the working fluid selection should be directly integrated into the design process of any ORC system. A direct formulation of the integrated design problem as mixed integer nonlinear program (MINLP) introduces one discrete degree of freedom for each considered working fluid resulting in a prohibitive problem size and complexity. Such an integrated design approach is therefore missing today for the design of ORCs.

Conceptually, the problem of selecting an ORC working fluid is strongly related to the design of a solvent for a separation problem. The definition of target properties for solvents is highly nontrivial due to the strong interaction between the solvent properties and the process. Approaches aiming for integrated solvent and process design have therefore been proposed.[12−16]

In the present study, we present a holistic framework for the selection of the working fluid and of key process parameters of Organic Rankine Cycles in one optimization problem. The presented framework builds upon the continuous-molecular targeting (CoMT-CAMD) concept recently introduced by the authors for integrated solvent design.[15] The integrated design of working fluid and ORC process is achieved by exploiting a physical meaningful model for the working fluid. For this purpose, we employ and extend the perturbed chain statistical associating fluid theory (PC-SAFT) equation. The framework also allows us to evaluate directly how the working fluid properties act on the optimal process performance. The method is demonstrated for a geothermally driven ORC.

The paper is structured as follows: in section 2, the current two-step approach for ORC design is briefly reviewed. Our framework for the integrated working fluid selection and process optimization is introduced in section 3. PC-SAFT is extended as a model for the working fluid in section 4. In section 5, the framework is applied to a case study and the

Received: February 14, 2014
Revised: April 23, 2014
Accepted: May 5, 2014
Published: May 5, 2014

   dx.doi.org/10.1021/ie5006542 | *Ind. Eng. Chem. Res.* 2014, 53, 8821−8830

results are analyzed in order to assess how the properties of the working fluid act on the process performance. Conclusions are drawn in section 6.

2. ORGANIC RANKINE CYCLE DESIGN

The design of an ORC for a specific application consists of two major parts: the selection of a working fluid and the optimization of the process variables (e.g., pressure levels, flow rates, size of the components). Today, these two design elements are usually addressed separately in a two-step approach (Figure 1).

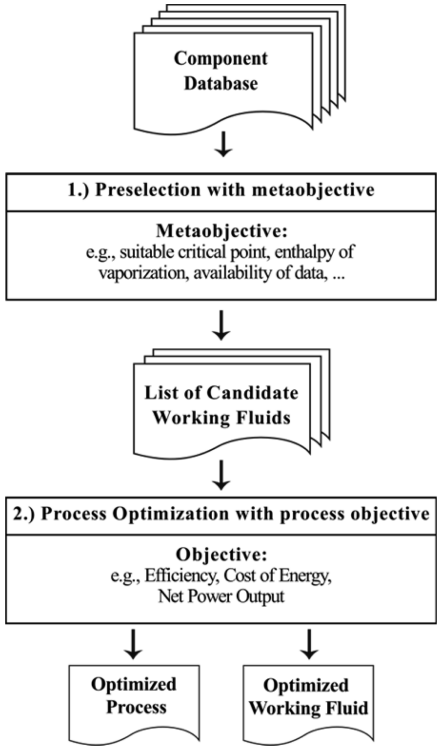

Figure 1. Established two-step approach for the design of ORCs.

A typical design protocol consists of a preselection step, where a component database is screened for working fluid candidates.[1,2,17] The candidates are selected by heuristically defined criteria (e.g., expected optimal critical point, enthalpy of vaporization, or availability of thermophysical property data). The preselection step results in a list of candidate working fluids. The list is limited to a reasonable number of working fluids to be assessed.[20] In the second step, for each candidate working fluid, the process performance is evaluated using simulation[2,3] or optimization.[21] The working fluid yielding the best objective function value will be selected.

The two-step approach relies on the definition of a *metaobjective* for the screening of a database. However, the use of a metaobjective bears the risk that promising candidates—and even the optimal fluid—are discarded if the heuristics underlying the metaobjective fail. The definition of a metaobjective for the preselection of working fluid candidates requires the engineer to decide a priori which thermophysical properties are most important for process performance and what values of these parameters are desirable. Even a qualitative definition of a metaobjective can be difficult and ambiguous, because changes in a specific parameter usually influence different parts of the ORC process simultaneously leading to complex trade-offs. Stijepovic et al.[8] have shown that the change in the thermophysical properties of the working fluid can positively affect one part of the cycle while adversely affecting another part. Their insightful study on ORCs identified several such trade-offs.

According to such trade-offs, the use of more than one thermophysical property in the definition of the metaobjective has been proposed. For this reason, the Jacob number ($Ja = c_pT/\Delta h_{evap}$) has been recommended for selecting a working fluid. The Jacob number reflects the trade-off between sensible and isothermal heat transfer and was found to correlate well with the thermal efficiency of the cycle.[22,23] However, the upper and lower temperature levels of the cycle are needed as input for the calculation. The temperatures in the cycle in turn depend on the working fluid used, and they are thus a result of a process optimization. Thus, a metaobjective based on the Jacob number requires a priori assumptions about the desired process. Due to these limitations, Quoilin et al.[11] recommend avoiding a preselection of working fluids and integrating the working fluid selection directly into the design of the process.

In their pioneering work, Papadopoulos et al.[6] introduced methods to avoid the preselection of candidates by using computer-aided molecular design (CAMD) and multi-objective optimization (MOO). CAMD methods aim at solving the inverse problem of the property prediction to identify molecular structures, which lead to desirable macroscopic properties.[19] The MOO allows to account for more than one property or metaobjective as objective function. In a more recent work on the design of working fluid mixtures,[18] the same authors show that the use of process-related objective functions (thermal and exergetic efficiency) in their design approach is possible. The calculation of these process-related objective functions is achieved by applying a cubic equation of state and a process model. The authors clearly demonstrate the merits of a design approach for ORC incorporating both working fluid and process. In the presented work, we show a general concept for a holistic design framework allowing for a simultaneous optimization of working fluid and process based on the physically meaningful PC-SAFT equation of state.

3. HOLISTIC DESIGN FRAMEWORK

The simultaneous optimization of working fluid and ORC process (Figure 2) begins with the typical specifications of the

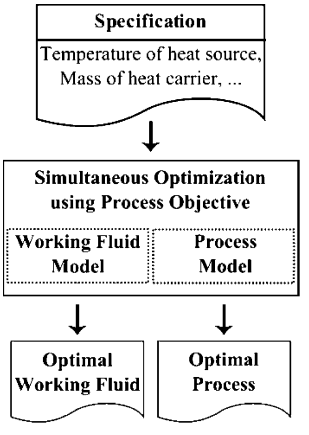

Figure 2. Simultaneous optimization of the working fluid and the process.

dx.doi.org/10.1021/ie5006542 | Ind. Eng. Chem. Res. 2014, 53, 8821−8830

ORC application. These specifications lead to the definition of constraints and parameters in the process optimization. The simultaneous optimization requires a model for both the process and the working fluid properties. Thereby, the working fluid and process conditions can be optimized with the same objective function; the definition of heuristics for preselecting a working fluid is overcome. The solution is an optimal pair of working fluid and process parameters. Such a simultaneous optimization directly captures all trade-offs between the process and the working fluid properties. A direct mathematical formulation of the simultaneous optimization problem leads to a MINLP of prohibitive size and complexity, because a discrete degree of freedom is added to the problem for each working fluid.[19] A method that still enables the simultaneous optimization is introduced in the following.

In our approach, the working fluid is represented by a thermodynamic model (Figure 3). Herein, the working fluid

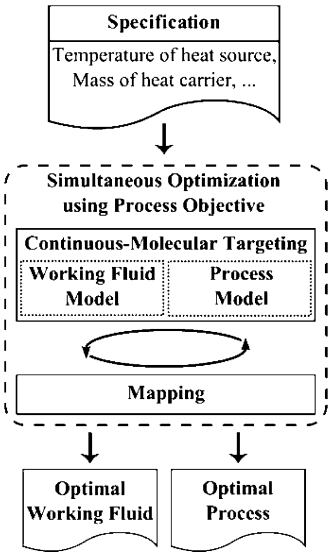

Figure 3. Framework for simultaneously optimizing process conditions and working fluid. The scheme shows the continuous-molecular targeting step and the mapping step.

properties are defined by a set of pure component parameters. The working fluid model employed in the presented framework is PC-SAFT (see section 4). PC-SAFT is a model for the residual Helmholtz energy and thus gives a consistent picture of all equilibrium properties of the working fluid. The simultaneous optimization of the working fluid and the process is enabled by relaxation of the pure component parameters for the working fluid in PC-SAFT from their discrete to continuous values. The relaxation allows for a simple gradient-based optimization of the objective function with respect to both the pure component parameters and process conditions. The result of the optimization, the so-called continuous-molecular targeting, is an optimal process and an optimal, hypothetical working fluid described by its PC-SAFT pure component parameters. Since these parameters usually do not coincide with a real fluid, real working fluids with similar properties are identified in the subsequent so-called mapping. The continuous-molecular targeting concept has been introduced by the authors for the simultaneous solvent and process design.[15] In a conference paper the authors already sketched the presented method for ORC processes and used it for the selection of working fluids from a single homologous series.[24] The individual parts of the framework are described in the following in more detail.

3.1. Continuous-Molecular Targeting. In PC-SAFT, the properties of a pure component are entirely defined by a vector y of pure component parameters, each specifying molecular attributes of the component, such as van der Waals attraction or hydrogen-bonding energy. In the suggested approach, the pure component parameters are relaxed from discrete to continuous values to allow for a simultaneous optimization. The relaxation of the pure component parameters transforms the mathematical problem of integrated working fluid and process design into a nonlinear program (NLP) solvable with standard solvers. The resulting problem consists of two types of variables: the vector y of pure component parameters and a vector x of key process parameters. The NLP formulation

$$\min_{x,y} f(x, y) \tag{1}$$

s.t.

$$g(x, y) \leq 0 \tag{2}$$

$$h(x, y) \leq 0 \tag{3}$$

$$x_{\min} \leq x \leq x_{\max} \tag{4}$$

$$y_{\min} \leq y \leq y_{\max} \tag{5}$$

allows for an optimization of the objective function $f(x,y)$. The formulation in eqs 1−5 has two sets of constraints: The set $g(x,y)$ contains the model of the process itself, while $h(x,y)$ contains the PC-SAFT equations. For the ORC process, any model based on thermophysical equilibrium properties can be used in the current implementation of the framework. The proposed approach allows for different objective functions, constraints, and specifications. Discrete design decisions (e.g., use of regeneration) could directly be integrated into the process model by introducing binary variables. The process model used in this work is a basic ORC for a geothermal application (see section 5.1). For this application, the optimized variables x are the working fluid flow rate, pressure levels, and temperatures in the cycle.

The problem of introducing discrete degrees of freedom to describe the working fluid in a simultaneous optimization is overcome. The pure component parameters of the working fluid and the process conditions are degrees of freedom on an equal footing to the optimization. A simple (gradient-based) optimization leads to the identification of the optimal pure component parameters y^* along with the optimal process parameters x^*. This step is called the *continuous-molecular targeting* (CoMT) step as it yields optimal pure component parameters representing a hypothetical, optimal target working fluid. In general, the hypothetical fluid does not coincide with a real fluid. Thus, the optimal working fluid properties are usually not achievable in practice, but the results of the CoMT optimization provide an upper bound for the performance of the process. Should the optimal process not be viable even with the hypothetical working fluid, no real working fluid will lead to a better performance.

To perform a CoMT optimization, bounds for the variables should be defined. The bounds $x_{\min}$ and $x_{\max}$ in eqs 1−5 are related to the process degrees of freedom and can be defined based on the specifications of the application. The bounds for the pure component parameters y are determined from a

dx.doi.org/10.1021/ie5006542 | Ind. Eng. Chem. Res. 2014, 53, 8821−8830

database. To identify real fluids with optimal performance, the optimal working fluid parameters are mapped onto a set d of known pure component parameters y_i in the mapping step (see section 3.2). The range of the parameters y_i in the database can, in turn, be used to constrain the search space of the pure component parameters in the CoMT optimization. For this purpose, a convex hull around the parameters y_i in d is used to define the allowable parameter range.[25,26] The convex hull can be modeled as a set of linear constraints

$$A(d)y - b(d) \leq 0 \tag{6}$$

where matrix A and vector b depend on the set d. Equation 6 ensures that the optimal fluid has pure component parameters within the limits defined by the database values.

In addition, if a set of constraints $g_s(y) \leq 0$ is independent of the process variables x, it can directly be assessed for fluids in the database. Based on these constraints, the database is refined before the convex hull is generated. g_s can contain constraints from g or be derived from g by elimination of process variables. For example, consider a subcritical cycle with the constraints $p_c > p_{evap} > p_{cond} \geq p_{min}$, where the evaporation pressure p_{evap} and the condensation pressure p_{cond} of the process depend on x, the minimal pressure p_{min} is a constant, and the critical pressure p_c is a function of y. Combining these constraints yields $p_c > p_{min}$, which is independent of x and can be added to g_s. The feasible components are gathered in the set d_{feas}, such that

$$d_{feas} = \{y_i \in d: g_s(y_i) \leq 0\} \tag{7}$$

Infeasible compounds are excluded from the database before the generation of the convex hull. The relevant parameter range of the PC-SAFT model is defined by the convex hull around the remaining, feasible substances in d_{feas}. Figure 4 shows the actual database used in the case study and the resulting feasible set by removing infeasible compounds. The feasible working fluids are contained in a region of the parameter space, where there are no infeasible working fluids in between them. Thus, the search space for the optimization is reduced. This behavior is not only useful from a numerical point of view but also demonstrates the strong physical nature of the underlying PC-SAFT model: The parameters directly relate to physical properties and vice versa, which is an important feature for the proposed design approach, as it can be exploited for relating the pure component parameters to real working fluids.

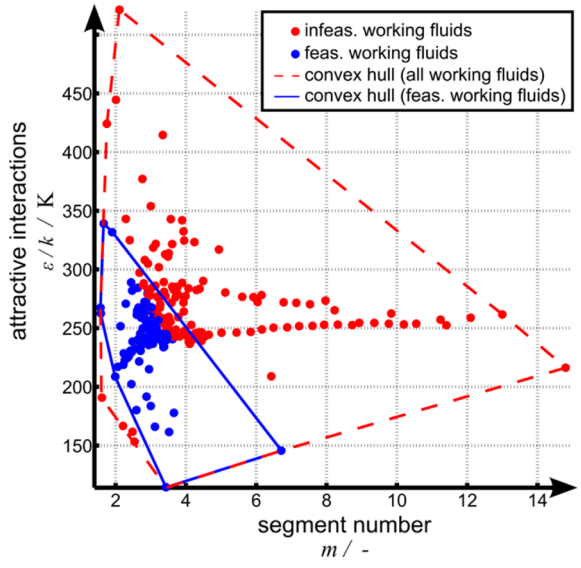

Figure 4. Convex hull constraints for two selected PC-SAFT parameters representing working fluid candidates. The dashed line is the convex hull around all pure component parameters (set d). The solid line is the refined convex hull around feasible pure components only (set d_{feas}, see text for details).

3.2. Mapping. The aim of the working fluid selection is to identify real working fluids that achieve the best possible performance. In this work, the pure component parameters of the optimal, hypothetical working fluid are mapped onto a database containing parameters of real working fluids. The components are ranked according to the expected loss in process performance compared to the best (hypothetical) working fluid. We employ a Taylor expansion of the objective function f for a fluid i with pure component parameters y_i around the optimal values y^*, as

$$\hat{f}(y_i) \approx f(y^*) + \frac{\partial f}{\partial y}(y_i - y^*) + (y_i - y^*)^T \frac{\partial^2 f}{\partial y^2}(y_i - y^*) \tag{8}$$

The estimate $\hat{f}$ can be evaluated efficiently for the complete database of pure component parameters. The estimates are used to generate a ranked list of candidate working fluids. This step is called *mapping*. The high-ranked working fluids are finally assessed in a process optimization to verify the predicted performance.

If the design of new working fluids is to be considered, CAMD methods[6] could be applied during the mapping to generate molecular structures with properties close to those of the hypothetical target fluid.

4. PC-SAFT AS WORKING FLUID MODEL

The CoMT-CAMD approach relies on the possibility to map optimized molecular parameters to a real substance. The molecular model of the PC-SAFT equation of state considers molecules as chains of spherical segments that interact through van der Waals interactions, hydrogen bonds, and polar interactions. Two parameters characterize the geometry of the molecule: the segment number m and a segment diameter parameter σ. The van der Waals attraction between segments is defined by a third parameter, the segment dispersion energy ε/k. In this work, these three parameters $y = (m, \sigma, \varepsilon/k)^T$ are used to describe the working fluid. The extension of the model to account for hydrogen bonding and polar interactions is straightforward.[15] It has been shown that interpretations of the parameters hold well. For example, for homologous series, linear relationships of the model parameters with chain length have been obtained.[27−29] PC-SAFT has already successfully been employed for the design of ORC systems.[30−33] For a detailed description of the PC-SAFT, the reader is referred to the original literature.[28,34−36]

PC-SAFT is a model for the residual Helmholtz energy of pure substances or mixtures. For calculating caloric properties (e.g., enthalpies), however, the ideal gas heat capacity is needed. In the ORC application, the ideal gas heat capacity strongly affects the process performance.[8] The influence of the ideal gas heat capacity on the ORC process design can be appreciated by comparing the two-phase regions of different working fluids. In Figure 5, the two-phase regions of three working fluids are shown in a temperature−entropy diagram. In Figure 5a, the ideal gas heat capacity is fixed for all components to $c_p^{ig,n\text{-pentane}}$,

dx.doi.org/10.1021/ie5006542 | Ind. Eng. Chem. Res. 2014, 53, 8821−8830

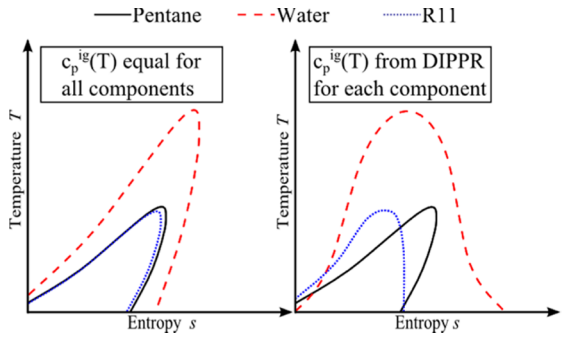

Figure 5. Two-phase regions for *n*-pentane, water, and R11 as predicted by PC-SAFT. (a, left) $c_p^{ig,pentane}$ is assumed for all components; (b, right) c_p^{ig} relations specific for each substance are used.[37]

while the pure component parameters of PC-SAFT change for all three working fluids. In Figure 5b) literature values[37] for c_p^{ig} for each component are employed. The ideal gas heat capacity substantially influences the shape of the two-phase region and thereby the ORC process performance.

When PC-SAFT is used for a known fluid, c_p^{ig} can be taken from a database. In our design setting, a novel fluid is only characterized by its PC-SAFT parameters. These parameters are therefore used to develop a quantitative structure−property relationship (QSPR) for the ideal gas heat capacity. A QSPR for estimating the ideal gas heat capacity is appealing in our approach, because not only the residual but also the full equilibrium properties of a component can then be obtained from PC-SAFT pure component parameters. This gives a consistent and sound model allowing for the working fluid selection. Furthermore, Figure 5 indicates that, without a calculation of the heat capacity, the set of pure component parameters could lead to degeneracy: All three parameters have qualitatively the same effect on the two-phase region in a temperature−entropy projection. This degeneracy emerges in our case, since the pressure behavior, which otherwise determines the pure component parameters uniquely, does not play an essential role here. Including the ideal gas properties through c_p^{ig} leads to a sound discrimination of the pure component parameters as shown below.

The ideal gas heat capacity for organic components is mainly determined by the energies associated with the translational, rotational, and vibrational degrees of freedom of the molecule.[38] For our expectation that a QSPR approach based on PC-SAFT parameters is promising, we can provide the following rationale: The energy stored in translation and rotation of the molecule depends on the size of the molecule, which is represented by the geometric parameters m and σ in PC-SAFT. The energy associated with vibrations within a molecule additionally depends on the magnitude of the forces between the atoms of the molecule, which, to some extent, scales with the segment dispersion energy ε/k. In the developed QSPR, the ideal gas heat capacity is calculated as a sum of structural descriptors p_i and coefficients a_i:

$$c_p^{ig,Pred} = \sum_{i=1}^{n} a_i p_i \tag{9}$$

The structural descriptors p_i are empirically derived from the pure component parameters and the temperature (Table 1). The coefficients are fitted to a set of approximately 500 pure components from the DIPPR database for 300 K and 400 K.

Table 1. Structural Descriptors p_i for the QSPR (eq 9) and Corresponding Coefficients a_i^{300} for T = 300 K and a_i^{400} for T = 400 K

i	p_i	a_i^{300}	a_i^{400}	unit [a_i]
1	1	-1.5×10^4	-1.9×10^4	J/(mol K)
2	$m(\varepsilon/(kT))$	-5.8×10^3	-8.2×10^3	J/mol
3	$m\sigma^3$	1.2×10^3	1.5×10^3	J/(mol K Å^3)
4	$m(\varepsilon/(kT))\sigma^3$	-2.4×10^2	-3.2×10^2	J/(mol Å^3)

The temperature dependency of c_p^{ig} is accounted for by linear interpolation between the two predicted values. The QSPR correlates the ideal gas heat capacity with a determination coefficient of 0.99 for both 300 K (Figure 6) and 400 K. A similar method is employed for the molecular mass of the working fluid.

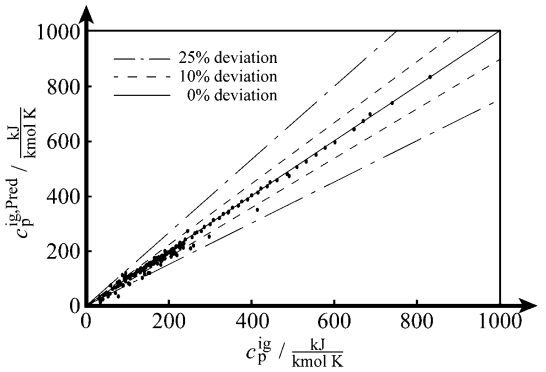

Figure 6. Literature values of the ideal gas heat capacity vs model predicted values from the QSPR for 300 K (eq 9).

The QSPR extends the PC-SAFT model such that it allows for the calculation of all static equilibrium properties of the working fluid, which is solely defined by its three pure component parameters. No additional parameters or properties are needed.

5. CASE STUDY

The CoMT-CAMD framework is applied to the optimization of a geothermal ORC for which the optimal working fluid and the optimal process conditions are determined. The specifications of the geothermal source (based on Heberle et al.[3]) are summarized in Table 2. We assume a fixed flow rate of heat carrier $\dot{m}_{HC}$ coming from the production drill hole with the temperature T_{HC}^{in} and a fixed heat capacity $c_{l,HC}$.

Table 2. Geothermal Source Specifications for the Case Study (Adopted from Ref 3)

parameter	symbol	value
heat carrier mass flow rate	$\dot{m}_{HC}$	66 kg/s
heat carrier inlet temperature	T_{HC}^{in}	120 °C
heat carrier heat capacity	$c_{l,HC}$	4200 J/kg K

5.1. Process Model. The process considered in this work is a basic ORC (Figure 7). Other ORC process models from the literature[2,10,39−41] could directly be used in the framework. The considered cycle consists of four parts: Between state points 1 and 2, the working fluid is *pumped* to pressure level p_{evap}. Between state points 2 and 3, the working fluid is preheated to the boiling point, evaporated, and optionally superheated. The

dx.doi.org/10.1021/ie5006542 | Ind. Eng. Chem. Res. 2014, 53, 8821−8830

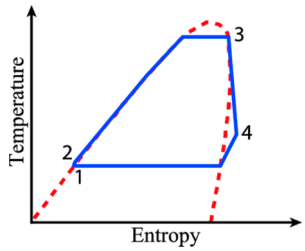

Figure 7. Simple ORC in a temperature−entropy chart.

vapor enters the *turbine* and work is extracted. After the turbine, the working fluid is in state 4 and enters the condenser, where the fluid is desuperheated and condensed to boiling liquid in state 1.

The objective is to maximize the net power output of the ORC, defined as the difference between the work of the turbine P_T and the work of the pump P_P, as

$$\max P_{net} = |P_T| - |P_P| \tag{10}$$

Neglecting the mechanical efficiencies of turbine and pump, the right-hand side of eq 10 can be expressed by energy balances around the pump and the turbine:

$$P_P = \dot{m}_{WF}(h_2 - h_1) \tag{11}$$

$$P_T = \dot{m}_{WF}(h_3 - h_4) \tag{12}$$

Using the assumption that the working fluid leaving the condenser is boiling liquid, the enthalpies in state 1 and state 3 are defined by $h_1 = h^{sat}(p_{cond})$ and $h_3 = h(p_{evap}, T^{sat}(p_{evap}) + \Delta T_{sh})$, respectively. The nonideal behaviors of pump and turbine are modeled by isentropic efficiencies η_P and η_T, respectively, where

$$\eta_P = \frac{h_2^* - h_1}{h_2 - h_1}; \qquad \eta_T = \frac{h_4 - h_3}{h_4^* - h_3} \tag{13}$$

with $h_2^* = h(p_{evap}, s_1)$ and $h_4^* = h(p_{evap}, s_3)$ being the states after an isentropic unit. The objective function is thus computed as

$$\begin{aligned} \max P_{net} &= \dot{m}_{WF}[-\eta_T(h_4^* - h_3) - \eta_P^{-1}(h_2^* - h_1)] \\ &= \dot{m}_{WF}[-\eta_T(h(p_{evap}, s_3) \\ &\quad - h(p_{evap}, T^{sat}(p_{evap}) + \Delta T_{sh})) \\ &\quad - \eta_P^{-1}(h(p_{evap}, s_1) - h^{sat}(p_{cond}))] \end{aligned} \tag{14}$$

The optimized variables in the process model are $x = (p_{cond}^{red}, p_{evap}^{red}, \Delta T_{sh}, \dot{m}_{WF})^T$: pressure of the condenser p_{cond}, pressure of the evaporator p_{evap}, degree of superheating ΔT_{sh}, and mass flow rate of the working fluid, $\dot{m}_{WF}$. As only subcritical processes are considered, reduced pressures are used as variables in the optimization (i.e., the pressure relative to the critical pressure p_c).

A minimal temperature difference in the evaporator ΔT_{min} is imposed to ensure feasible heat transfer (Table 3). Additionally, minimal and maximal allowed pressures p_{min} and p_{max} are defined. The pressure levels in the cycle are further constrained by minimal and maximal reduced pressures p_{min}^{red} and p_{max}^{red}, respectively. A minimal allowed temperature T_{min} is chosen to allow for cooling in the condenser.

The model is implemented in Fortran. The derivatives of the model needed during optimization are obtained from automatic differentiation using Adifor 2.0.[43]

Table 3. Specifications and Constraints for the Geothermal ORC

parameter	symbol	value
minimal temperature difference	ΔT_{min}	10 K
turbine efficiency	η_T	0.8
pump efficiency	η_P	0.6
minimal absolute pressure	p_{min}	1 bar
minimal reduced pressure	p_{min}^{red}	10^{-5}
maximal absolute pressure	p_{max}	20 bar
maximal reduced pressure	p_{max}^{red}	0.8
minimal temperature	T_{min}	20 °C

5.2. Results. We present results for maximizing the net power output of a geothermal ORC. In a preparatory step, the database of fluids is assessed for simple constraints and infeasible components are deleted, as discussed in section 3.1. The constraints g_s used for the refinement of the database are

$$\begin{aligned} &T_c - T_{min} \geq 0 \\ &p_c - p_{min} \geq 0 \\ &\max(p^{sat}(T_{HC}^{in}); p_c p_{max}^{red}) - p_{min} \geq 0 \\ &p_{max} - \min(p^{sat}(T_{min}); p_c p_{min}^{red}) \geq 0 \end{aligned} \tag{15}$$

These constraints ensure a subcritical cycle and the existence of feasible pressure levels. After the refinement, the convex hull around the feasible working fluids is defined. Figure 4 shows the actual result for the present case, thereby showing that simple constraints in process settings translate into clear regions in the parameter space.

The CoMT optimization with the relaxed pure component parameters is performed. The computations took less than 30 s on a standard desktop PC (Core i5 CPU 3.2 GHz with 4 GB RAM), demonstrating the advantage of avoiding discrete degrees of freedom. Table 4 shows the optimized variables. The result of the optimization is a subcritical cycle with no superheating. The net power output of the optimal cycle is 3.2 MW.

The result of the optimization is both an optimal process and an optimal hypothetic working fluid. This combination is the target for the following mapping. Using a Taylor approximation around the optimum (eq 8), the database of feasible fluids is assessed and ranked according to the expected net power output. The high-ranked working fluids are further assessed by a process optimization, where only the process degrees of freedom $x = (p_{cond}^{red}, p_{evap}^{red}, \Delta T_{sh}, \dot{m}_{WF})^T$ are optimized. Table 5 summarizes the results for the 10 working fluids ranked highest in the mapping.

In order to evaluate our optimization result, we have performed individual process optimizations for all 200 fluids in our database. The real ranking list ($\#_{Real}$) of the 200 substances is unambiguous and serves as a measure for how well the CoMT-CAMD method identifies the most optimal working fluids.

A rich set of promising working fluids is identified (Table 5). The highest-ranked working fluid in the mapping is dinitrogen tetraoxide. The prediction for this fluid is highest, but the actual performance is low. It should be noted that this component is actually not available in pure form due to its reactive nature at process conditions. The second- and third-ranked fluids (R124 and R227ea) are the actual best and second best fluids from the

dx.doi.org/10.1021/ie5006542 | Ind. Eng. Chem. Res. 2014, 53, 8821−8830

Table 4. Result of the Simultaneous Optimization of Working Fluid and Process[a]

variable	m	σ/Å	(ε/k)/K	p_{cond}^{red}	p_{evap}^{red}	$\dot{m}_{WF}$/kg s^{-1}	ΔT_{sh}/K	P_{net}/MW
optimal value	5.7	2.9	133	0.1	0.8*	65	0*	3.2

[a]Parameters at a bound are marked with an asterisk.

Table 5. Ranked List of the Most Promising Working Fluids from the Mapping Step ($\#_{Mapping}$) and Comparison to the Real Rank ($\#_{Real}$) and the Real Power Output, with the Pure Component Parameters (m, σ, and ε/k) Listed for Comparison

$\#_{Mapping}$	name	P_{net}/MW	$\#_{Real}$	m	σ/Å	(ε/k)/K
	target	3.2		5.7	2.9	133
1	dinitrogen tetraoxide	1.6	18	6.7	2.2	146
2	R1243	2.5	2	3.9	3.0	151
3	R227ea	2.7	1	3.5	3.3	162
4	R134a	2.1	6	3.1	3.1	166
5	R236ea	1.9	10	3.7	3.2	178
6	R152a	1.8	16	2.6	3.2	180
7	R124	2.1	4	3.0	3.3	184
8	cyanogen	0.2	41	2.9	2.9	192
9	R142b	2.1	5	2.5	3.5	202
10	propane	2.1	3	2.0	3.6	209

complete database. The optimal hypothetical working fluid and the optimal real working fluid R227ea are similar with respect to the shape of the two-phase region and the critical temperature (Figure 8). The predicted top 10 contains the

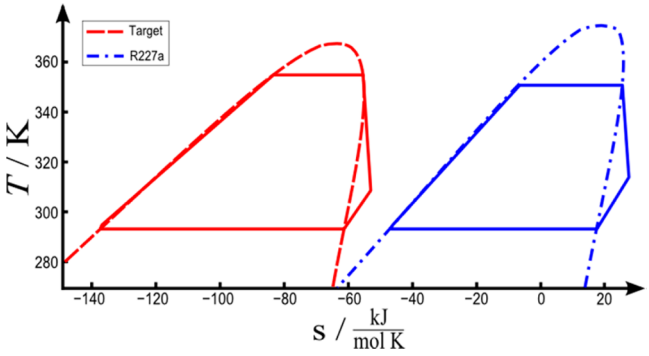

Figure 8. Optimal working fluid from the CoMT optimization (left) and the best working fluid (right) compared in a temperature−entropy chart.

top six fluids from the database. These fluids identified by the CoMT-CAMD approach can now be assessed for other properties that are not covered by the process optimization (e.g., toxicity, flammability, global warming potential, or legal prescriptions).[44,45]

The results from the mapping show that the new framework enables the selection of a working fluid and the optimization of the key process parameters in one optimization problem. However, some of the high-ranked working fluids in the mapping have low performance (e.g., dinitrogen tetroxide, cyanogen). The observed difference in the predicted and the actual performance can be explained by analyzing the process performance with respect to changes in the working fluid properties.

5.3. Influence of Working Fluid Properties on Process Performance. Process models of the ORC can provide insight into the influence of process parameters (e.g., pressure levels, temperature of the heat source) on the process performance.[2,3,20,42] The presented framework employs a holistic model of the ORC process by integrating a model of the working fluid into the process model. Thereby, this holistic model allows analyzing the influence of both process parameters and working fluid properties on the process performance. Thus, a detailed analysis of the influence of working fluid properties on the process performance is possible.

In Figure 9, the net power output P_{net} of the optimal process is shown as a function of the segment number m and the segment diameter σ. The segment energy ε/k is kept constant at the optimal value of 133 K. Each point of the surface represents a solution of

$$\max_x P_{net}(x, y) \tag{16}$$

s.t.

$$g(x, y) \leq 0 \tag{17}$$

$$h(x, y) \leq 0 \tag{18}$$

$$x_{min} \leq x \leq x_{max} \tag{19}$$

$$y = \text{const} \tag{20}$$

and, thus, an optimal process, where $x = (p_{cond}^{red}, p_{evap}^{red}, \Delta T_{sh}, \dot{m}_{WF})^T$ has its optimized value for each y. The surface has a distinct maximum at $m = 5.7$ and $\sigma = 2.9$ Å. The absence of flat regions of almost constant objective function values indicates that there is no degeneracy of the PC-SAFT parameters. Figure 9 only shows a two-dimensional cut of the design space; however, we have no indication that parameter degeneracy is a problem for the presented ORC design approach. The gradients and the curvature of the surface change drastically for different points of the surface. These abrupt changes in the gradient hinder an optimization of the model using finite differences. Convergence therefore improved significantly by using automatic differentiation to obtain exact gradients of the objective function and the constraints.

In Figure 9, regions are indicated representing different active sets of constraints. The active set is the subset of constraints, which are at their respective bounds for the optimal process (i.e., $g_i(x^*,y) = 0$). The active constraints in the different regions are the maximal absolute pressure, the pinch at the preheater entry, and the pinch at the evaporator entry. The different active constraints determine how changes in the fluid parameters act on the objective function. As a result, one can observe that the gradients and curvature change abruptly, when a switchover of one to the other active set is reached. For small values of the segment number m, the net power output is rising for rising m, until the pinch at the preheater entry is reached. When the new constraint becomes active, a sharp drop of the net power output can be observed. Changes in the working fluid properties affect the cycle in many different ways, and the active constraints are not known in advance. These observations show that metaobjective functions intended to guide the selection of working fluids are difficult to develop a priori and require a deep understanding of the process. The

dx.doi.org/10.1021/ie5006542 | Ind. Eng. Chem. Res. 2014, 53, 8821−8830

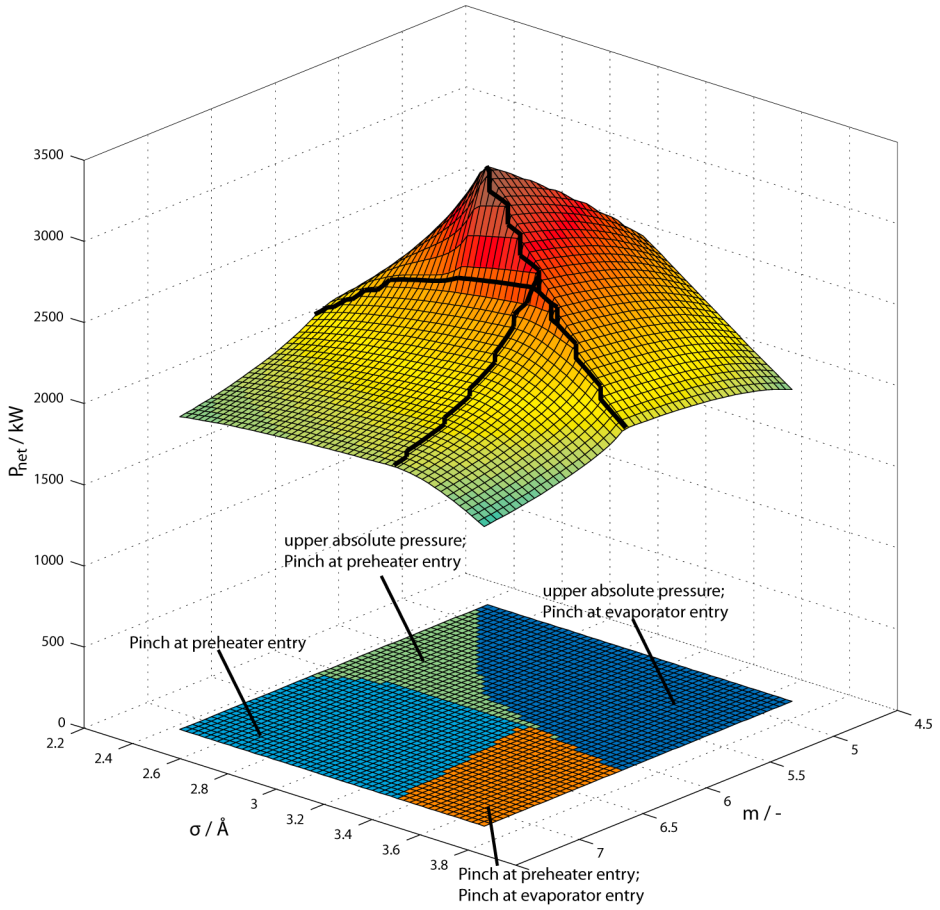

Figure 9. Optimal net power output as a function of the segment number m and the segment diameter σ for constant segment dispersion energy ε/k = 133 K. The projected regions on the bottom represent different active sets of constraints.

appearance of many faces in the objective function (Figure 9) clearly shows the limitations of metaobjective functions, and we thus interpret Figure 9 as supporting the integrated optimization of working fluid and process parameters.

The Taylor approximation (eq 8) employed for the mapping does not account for changes in the active set. The insight gained by Figure 9 enables us to explain the appearance of dinitrogen tetroxide high in the ranking list: Fluids that are overestimated in the mapping can be expected when the set of active constraints changes along the path of the Taylor expansion. To account for the changes of the active set in the mapping could be a further refinement of the method. However, the results show that the list of high-ranked fluids from the current mapping already gives a rich set of good fluid candidates that can be assessed further.

6. CONCLUSIONS

A framework for the holistic design of an ORC is presented, where the selection of a working fluid and the optimization of the process are integrated into a single optimization problem. The presented CoMT-CAMD framework has successfully been applied to optimizing an ORC for a geothermal application. The method was used to generate a ranking list of the 10 most promising working fluids out of a database of 200 substances. The net power output was considered as the only objective function. No heuristics were considered. A rigorous optimization was run for the 200 substances in order to unambiguously assess the proposed ranking list. It was seen that the top six working fluids were indeed members of the CoMT-CAMD (top 10) ranking list.

A subsequent analysis of the objective function showed kinks in the surface of the objective function, caused by the switchover from one set of active process constraints to another. These kinks in the objective function surface are responsible for some less-promising working fluids entering the ranking list. At the same time, the kinks explain why heuristics or metaobjectives can only be applicable in small ranges (in fact, ranges unknown a priori) of working fluid properties.

For the ORC process, it was essential to supplement the PC-SAFT equation of state with a good predictor of the heat capacity $c_p^{ig}(T)$ of substances in the ideal gas state. More specifically, it is required that $c_p^{ig}(T)$ can be estimated from the pure component parameters of the PC-SAFT model only. A QSPR for the ideal gas heat capacity was developed with a determination coefficient of 0.99 for eight parameters adjusted to 500 pure components. The new relation for the ideal gas contribution to the heat capacity broadens the applicability of the presented CoMT-CAMD approach to many other applications.

AUTHOR INFORMATION

Corresponding Author

*E-mail: andre.bardow@ltt.rwth-aachen.de.

Notes

The authors declare no competing financial interest.

REFERENCES

(1) Wang, Z.; Zhou, N.; Guo, J.; Wang, X. Fluid selection and parametric optimization of organic Rankine cycle using low temperature waste heat. *Energy* **2012**, *40* (1), 107−115.

(2) Tchanche, B. F.; Papadakis, G.; Lambrinos, G.; Frangoudakis, A. Fluid selection for a low-temperature solar organic Rankine cycle. *Appl. Therm. Eng.* **2009**, *29* (11−12), 2468−2476.

(3) Heberle, F.; Brüggemann, D. Exergy based fluid selection for a geothermal Organic Rankine Cycle for combined heat and power generation. *Appl. Therm. Eng.* **2010**, *30* (11−12), 1326−1332.

(4) Siddiqi, M.; Atakan, B. Investigation of the Criteria for Fluid Selection in Rankine Cycles for Waste Heat Recovery. *Int. J. Thermodyn.* **2011**, *14* (3), 117−123.

(5) Saleh, B.; Koglbauer, G.; Wendland, M.; Fischer, J. Working fluids for low-temperature organic Rankine cycles. *Energy* **2007**, *32* (7), 1210−1221.

(6) Papadopoulos, A. I.; Stijepovic, M.; Linke, P. On the systematic design and selection of optimal working fluids for Organic Rankine Cycles. *Appl. Therm. Eng.* **2010**, *30* (6−7), 760−769.

(7) Quoilin, S.; Declaye, S.; Tchanche, B. F.; Lemort, V. Thermo-economic optimization of waste heat recovery Organic Rankine Cycles. *Appl. Therm. Eng.* **2011**, *31* (14−15), 2885−2893.

(8) Stijepovic, M. Z.; Linke, P.; Papadopoulos, A. I.; Grujic, A. S. On the role of working fluid properties in Organic Rankine Cycle performance. *Appl. Therm. Eng.* **2012**, *36*, 406−413.

(9) Borsukiewicz-Gozdur, A. Pumping work in the organic Rankine cycle. *Appl. Therm. Eng.* **2013**, *51* (1−2), 781−786.

(10) Chen, H.; Goswami, D. Y.; Stefanakos, E. K. A review of thermodynamic cycles and working fluids for the conversion of low-grade heat. *Renewable Sustainable Energy Rev.* **2010**, *14* (9), 3059−3067.

(11) Quoilin, S.; Broek, M. V. D.; Declaye, S.; Dewallef, P.; Lemort, V. Techno-economic survey of Organic Rankine Cycle (ORC) systems. *Renewable Sustainable Energy Rev.* **2013**, *22*, 168−186.

(12) Hostrup, M.; Harper, P. M.; Gani, R. Design of environmentally benign processes: integration of solvent design and separation process synthesis. *Comput. Chem. Eng.* **1999**, *23*, 1395−1414.

(13) Eden, M. R.; Jorgensen, S. B.; Gani, R.; El-Halwagi, M. M. A novel framework for simultaneous separation process and product design. *Chem. Eng. Process.* **2004**, *43*, 595−608.

(14) Papadopoulos, A. I.; Linke, P. Integrated solvent and process selection for separation and reactive separation systems. *Chem. Eng. Process.* **2009**, *48*, 1047−1060.

(15) Bardow, A.; Steur, K.; Gross, J. Continuous-Molecular Targeting for Integrated Solvent and Process Design. *Ind. Eng. Chem. Res.* **2010**, *49* (6), 2834−2840.

(16) Pereira, F. E.; Keskes, E.; Galindo, A.; Jackson, G.; Adjiman, C. S. Integrated solvent and process design using a SAFT-VR thermodynamic description: High-pressure separation of carbon dioxide and methane. *Comput. Chem. Eng.* **2011**, *35* (3), 474−491.

(17) Kosmadakis, G.; Manolakos, D.; Kyritsis, S.; Papadakis, G. Comparative thermodynamic study of refrigerants to select the best for use in the high-temperature stage of a two-stage organic Rankine cycle for RO desalination. *Desalination* **2009**, *243* (1−3), 74−94.

(18) Papadopoulos, A. I.; Stijepovic, M.; Linke, P.; Seferlis, P.; Voutetakis, S. Toward Optimum Working Fluid Mixtures for Organic Rankine Cycles using Molecular Design and Sensitivity Analysis. *Ind. Eng. Chem. Res.* **2013**, *52*, 12116−12133.

(19) Gani, R.; Achenie, L. E. K.; Venkatasubramanian, V. Introduction to CAMD. In *Computer Aided Molecular Design: Theory and Practice*; Achenie, L. E. K., Gani, R., Venkatasubramanian, V., Eds.; Elsevier: Amsterdam, The Netherlands, 2003; pp 3−21.

(20) Quoilin, S.; Declaye, S.; Tchanche, B. F.; Lemort, V. Thermo-economic optimization of waste heat recovery Organic Rankine Cycles. *Appl. Therm. Eng.* **2011**, *31* (14−15), 2885−2893.

(21) Wei, D.; Lu, X.; Lu, Z.; Gu, J. Performance analysis and optimization of organic Rankine cycle (ORC) for waste heat recovery. *Energy Convers. Manage.* **2007**, *48*, 1113−1119.

(22) Mikielewicz, D.; Mikielewicz, J. A thermodynamic criterion for selection of working fluid for subcritical and supercritical domestic micro CHP. *Appl. Therm. Eng.* **2010**, *30* (16), 2357−2362.

(23) Kuo, C.-R.; Hsu, S.-W.; Chang, K.-H.; Wang, C.-C. Analysis of a 50 kW organic Rankine cycle system. *Energy* **2011**, *36* (10), 5877−5885.

(24) Lampe, M.; Gross, J.; Bardow, A. Simultaneous process and working fluid optimization for Organic Rankine Cycles (ORC) using PC-SAFT. In *Proceedings of the 22nd European Symposium on Computer Aided Process Engineering, June 17−20, 2012, London*; Bogle, I. D. L., Fairweather, M., Eds.; Elsevier: Amsterdam, The Netherlands, 2012.

(25) Knuth, D. *Axioms and Hulls*; Lecture Notes in Computer Science 606; Springer-Verlag: Heidelberg, Germany, 1992.

(26) Barber, C. B.; Dobkin, P. D.; Huhdanpaa, H. The Quickhull Algorithm for Convex Hulls. *ACM Trans. Math. Software* **1996**, *22* (4), 469−483.

(27) Pedrosa, N.; Vega, L. F.; Coutinho, J. A. P.; Marrucho, I. M. Phase Equilibria Calculations of Polyethylene Solutions from SAFT-Type Equations of State. *Macromolecules* **2006**, *39* (12), 4240−4246.

(28) Gross, J.; Sadowski, G. Perturbed-Chain SAFT: An Equation of State Based on a Perturbation Theory for Chain Molecules. *Ind. Eng. Chem. Res.* **2001**, *40* (4), 1244−1260.

(29) Nannan, N. R.; De Servi, C. M.; van der Stelt, T.; Colonna, P.; Bardow, A. An Equation of State Based on PC-SAFT for Physical Solvents Composed of Polyethylene Glycol Dimethylethers. *Ind. Eng. Chem. Res.* **2013**, *52* (51), 18401−18412.

(30) Lai, N. A.; Wendland, M.; Fischer, J. Description of linear siloxanes with PC-SAFT equation. *Fluid Phase Equilib.* **2009**, *283* (1−2), 22−30.

(31) Lai, N. A.; Wendland, M.; Fischer, J. Working fluids for high-temperature organic Rankine cycles. *Energy* **2011**, *36* (1), 199−211.

(32) Oyewunmi, O.; Taleb, A.; Haslam, A.; Markides, C. An Assessment of Working-Fluid Mixtures in Organic Rankine Cycles for Waste-Heat Recovery using SAFT-VR. Presented at the 2nd International Seminar on ORC Power Systems, 2013. Abstract retrieved from http://www.asme-orc2013.nl/program/show_slot/22.

(33) Vatani, A.; Khazaeli, A.; Roshandel, R.; Panjeshahi, M. H. Thermodynamic analysis of application of organic Rankine cycle for heat recovery from an integrated DIR-MCFC with pre-reformer. *Energy Convers. Manage.* **2013**, *67*, 197−207.

(34) Gross, J.; Vrabec, J. An equation-of-state contribution for polar components: Dipolar molecules. *AIChE J.* **2006**, *52* (3), 1194−1204.

(35) Vrabec, J.; Gross, J. Vapor−Liquid Equilibria Simulation and an Equation of State Contribution for Dipole−Quadrupole Interactions. *J. Phys. Chem. B* **2008**, *112* (1), 51−60.

(36) Gross, J. An equation-of-state contribution for polar components: Quadrupolar molecules. *AIChE J.* **2005**, *51* (9), 2556−2568.

(37) Rowley, R. L.; Wilding, W. V.; Oscarson, J. L.; Yang, Y.; Zundel, N. A.; Daubert, T. E.; Danner, R. P. *DIPPR Data Compilation of Pure Chemical Properties*; Design Institute for Physical Properties, Brigham Young University: Provo, UT, 2006.

(38) Coniglio, L.; Daridon, J. A group contribution method for estimating ideal gas heat capacities of hydrocarbons. *Fluid Phase Equilib.* **1997**, *139* (1−2), 15−35.

(39) Maizza, V.; Maizza, A. Unconventional working fluids in organic Rankine-cycles for waste energy recovery systems. *Appl. Therm. Eng.* **2001**, *21* (3), 381−390.

(40) Wang, D.; Ling, X.; Peng, H. Performance analysis of double organic Rankine cycle for discontinuous low temperature waste heat recovery. *Appl. Therm. Eng.* **2012**, *48*, 63−71.

(41) Mago, P. J.; Chamra, L. M.; Srinivasan, K.; Somayaji, C. An examination of regenerative organic Rankine cycles using dry fluids. *Appl. Therm. Eng.* **2008**, *28* (8−9), 998−1007.

(42) Vetter, C.; Wiemer, H.-J.; Kuhn, D. Comparison of sub- and supercritical Organic Rankine Cycles for power generation from low-temperature/low-enthalpy geothermal wells; considering specific net power output and efficiency. *Appl. Therm. Eng.* **2013**, *51* (1−2), 871−879.

(43) Bischof, C.; Khademi, P.; Mauer, A.; Carle, A. Adifor 2.0: automatic differentiation of Fortran 77 programs. *IEEE Comput. Sci. Eng.* **1996**, *3* (3), 18−32.
(44) Kazakov, A.; McLinden, M. O.; Frenkel, M. Computational Design of New Refrigerant Fluids Based on Environmental, Safety, and Thermodynamic Characteristics. *Ind. Eng. Chem. Res.* **2012**, *51* (38), 12537−12548.
(45) Andersen, W. C.; Bruno, J.; Rapid, T. J. Screening of Fluids for Chemical Stability in Organic Rankine Cycle Applications. *Ind. Eng. Chem. Res.* **2005**, *44* (15), 5560−5566.